SLAC-PUB-1481
September 1974
(T/E)

SEARCH FOR BACKWARDS-PRODUCED EXOTIC MESON RESONANCES IN 8.4 GeV/c $\pi^+ p$ INTERACTIONS*

M. S. Alam, B. B. Brabson, K. Galloway, R. Mercer
Indiana University, Bloomington, Indiana 47401

and

N. V. Baggett, E. C. Fowler, M. L. Huebschman, A. E. Kreymer
Purdue University, Lafayette, Indiana 47907

and

A. H. Rogers
Stanford Linear Accelerator Center
Stanford, California 94305

and

C. Baglin†, J. Hanlon, R. Kamat, R. Panvini, E. Petraske,
S. Stone, J. Waters, M. Webster
Vanderbilt University, Nashville, Tennessee 37203

Results are reported from a hybrid experiment designed to search for backwards-produced charge = +2 exotic meson resonances by investigating the reaction $\pi^+ + p \rightarrow X^{++} + n$(forward) at 8.4 GeV/c. The data reported here correspond to approximately 30 events per microbarn. No clear evidence for narrow exotic mesons was found for masses ≤ 3.0 GeV in the decay modes accessible for study which included: $X^{++} \rightarrow \pi^+\pi^+$, $\pi^+\pi^+\pi^+\pi^-$, $\pi^+\pi^+\pi^+\pi^+\pi^-\pi^-$, and $\bar{p}p\pi^+\pi^+$.

(Submitted to Physics Letters B)

*Work supported by the National Science Foundation and the U.S. Atomic Energy Commission.

†Senior postdoctoral fellow on leave from École Polytechnique.

We report on a search for backwards-produced exotic meson resonances in the baryon exchange reaction

$$\pi^+ + p \rightarrow X^{++} + n(\text{forward}) \qquad (1)$$

at 8.4 GeV/c incident π^+ momentum. An isospin-two charge-two X^{++} resonance would be exotic since it could not fit into a SU(3) multiplet with as few as one or eight members, as do all observed meson states. In a quark model, it would have to be made of at least two quarks and two antiquarks, unlike all observed meson states which can be constructed from a single quark-antiquark pair.

Since reaction (1) involves a virtual $\overline{\Delta^{=}}$ p interaction at the proton vertex, it is an example of baryon-antibaryon scattering, which violates the rules of two-component duality unless exotic X^{++} resonances exist.[1] Moreover, from duality considerations, meson resonances in the X^{++} system of reaction (1) should be produced with approximately the same cross sections as non-exotic meson resonances in backward-production reactions such as $\pi^- + p \rightarrow X^- + p(\text{forward})$. Evidence for ρ^- and possible A_1^- and A_2^- resonances in the X^- system has been seen[2] for 8 and 16 GeV/c incident pions. At 8 GeV/c the cross sections are approximately one microbarn for each resonance, implying that we might expect a production cross section of that order in the X^{++} system.

To investigate reaction (1), we combined a downstream neutron detector with the newly completed 15-inch rapid cycling bubble chamber (RCBC) at the Stanford Linear Accelerator Center (SLAC); see Fig. 1.

The bubble chamber had an analyzing magnetic field of 18,000 Gauss, and photographs were taken only for events satisfying the master trigger, which was defined as $B_1 \cdot B_2 \cdot \bar{A}_c \cdot \bar{A}_\gamma \cdot (N_1 \cdot N_2 + N_2 \cdot N_3 + N_3 \cdot N_4) \cdot \bar{A}_b$. This corresponds to a beam track which passes through B_1 and B_2 and then interacts in the bubble chamber in such a way that a neutral particle (neutron, anti-neutron, K^o, or $\bar{K}^o$) is projected forward within an angle of about 9^o relative to the beam direction. If in the same event charged secondary particles or gamma rays from π^o decays lie within this 9^o, the event is vetoed by counters A_c and A_γ. A_b vetoes non-interacting beam particles. Finally, the neutral particles interacting in the Spark Chambers must produce charged particles with sufficient energy to traverse two successive "neutron" (N) counters.

All interactions within a fiducial volume of 23 cm length in the bubble chamber were scanned and measured. Results are reported from a total of 74,000 bubble chamber triads, trigger-selected from about 1.1×10^7 expansions, with an average of 10 beam tracks per picture. The effective statistical level, accounting for the triggering requirements, is about 30 events per microbarn. All tracks in the bubble chamber, including events with Vees pointing to the primary vertex, were geometrically reconstructed with a standard three view geometry program (TVGP). From the measured momenta of the charged tracks in each event a missing momentum was computed. Events with missing momentum greater than 3 GeV/c were considered candidates for spark chamber measurement. Accordingly, 17,000 events measured in the bubble chamber were reduced to about 8,000 events after the 3 GeV/c cut. Finally, a total of 5,300 events were actually measured in the spark chamber film after imposing additional rules for defining the point of interaction of the neutral in the spark chambers. Thus, two samples of event were left for further analysis, those with and those without accompanying spark chamber measurements.

We applied three kinds of selection criteria to isolate the final states where $X^{++} \to 2\pi^+, 4\pi^\pm, 6\pi^\pm$: (1) The cross sections of these final states were estimated by computing the missing mass and fitting a gaussian to a neutron peak above a smooth background. (2) A second procedure involved making one-constraint (1C) fits to these channels. In spite of possible ambiguities in the 1C fits due to short track lengths, if there were a narrow resonance in these channels it would show up as a sharp bump above a background including misinterpreted events. Two levels of 1C fits were applied. At one level we accepted every event that had a χ^2 probability above ~ 4%. The more restrictive level of 1C fits involved these additional requirements: the χ^2 probability for the desired final state must be $\geq$ 10 times the χ^2 probability for the next best fit having a different interpretation, and the missing mass squared must lie within the broad limits $-1.0 < MM^2 < 3.0$ GeV^2. (3) Finally, in the subsample of events where the neutron direction was successfully determined by downstream spark chamber measurements, three constraint (3C) fits were made.*

Another check of our analysis procedures was made by measuring the cross sections of reactions already measured in other experiments. For this purpose, incident protons were used to study the reaction $pp \to \Delta^{++}n$. Also, in the main portion of our run, the reaction

$$\pi^+ + p \to \underset{\lfloor\!\to \Lambda^0\pi^+}{Y^{*+}(1388)} + \underset{\lfloor\!\to K^0\pi^+}{K^{*+}(890)}$$

was observed. Our Monte Carlo simulation program, which incorporated triggering requirements and geometrical acceptance, was tested by applying it to these two comparison reactions. The previously measured cross sections[3] for the $pp \rightarrow \Delta^{++}n$ and $\pi^{+}p \rightarrow Y^{*} K^{*}$ reactions at our energy are 675 ± 225 μb and 10 ± 5 μb, respectively. Our values are 560 ± 280 μb and 10 ± 4 μb, including both statistical and systematic uncertainties. Since we are searching for relatively gross effects, the agreement indicated by the above comparisons is sufficient to warrant confidence in our overall procedures.

Invariant mass spectra for the 2π, 4π and 6π channels, obtained from the 1C fits, are shown in Figs. 2(a), (b) and (c), respectively. The solid histograms represent the more inclusive sample and the dashed histograms are those with the additional cuts, as described previously. The smooth curves on these histograms are low order polynominals ($\leq$ 6th order), which in all cases fit the data with greater than 60% χ^2 probability. We interpret these good fits to the mass distribution as quantitative evidence that no narrow resonances, $\lesssim$ 100 MeV, are seen in the data.**

Narrow resonances with large enough cross section would be seen as sharp deviations from the smooth curves in Fig. 2. To compute upper limits for resonance production, we define a number, N, such that

$$N - 4\sqrt{N} = n$$

where n is the number of events in a 100 MeV bin at the level of the smooth curve in the upper (solid) histograms of Fig. 2. N is the number of events that would have been obtained if there were a narrow resonance above background, and n were a four standard deviation fluctuation downward. Thus, N-n, when converted to a cross section, represents an upper limit on 100 MeV wide resonance production. Figure 3 shows this upper limit in microbarns as a function of the X^{++} mass. The curves in this figure do not include error bars but a 50% systematic uncertainty should be understood. The upper limit is seen to be $\sim 1 - 2$ μb per 100 MeV interval.

The 3C fits were used for studying the overall shapes of the particle distributions since relatively few misinterpreted events are likely to be included in this sample. Mass spectra of these events are shown in Figs. 4(a), (b) and (c) for $X^{++} \to 2\pi, 4\pi, 6\pi$, respectively. The smooth curves shown were obtained from the Monte Carlo simulation of the data with the invariant phase space modified by the squared matrix element

$$|M|^2 \sim \prod_i \exp\left(-1.5(p_\perp)_i^2\right) .$$

The index i refers to each final state particle, including the neutron, and $(p_\perp)_i$ is just the transverse momentum of particle i. We have used the same matrix element for all three final states shown in the figure. The good qualitative agreement of the data with this simple modified phase space model can be interpreted as demonstrating that the mass spectra reveal no noteworthy dynamical features.***

In addition to the pion channels discussed above, we have analyzed the $(\bar{p}p\pi^+\pi^+) + n_{forward}$ final state in our data. This channel is of considerable interest since baryon-antibaryon decay modes of X^{++} might be expected to dominate. Since there are ambiguities with other channels, we rely on the three constraint fits to the $\bar{p}p\pi^+\pi^+$ final state and we require the kinematic chi-squared probability > 4%. A total of 18 events were found but only 3 were unique fits to this final state. The remainder of the events gave acceptable fits to other, more copiously produced channels, including those with K^+K^- instead of $\bar{p}p$ pairs or events with forward K^0's instead of neutrons. The 18 candidates had $\bar{p}p\pi^+\pi^+$ invariant masses between 2.45 and 3.5 GeV with no indication of an enhancement at any specific mass. Accounting for various corrections, the 3 unique events correspond to 0.2 microbarns and the 18 events to 1.3 microbarns.

We conclude by reiterating that the baryon exchange reaction (1) for production of charge-two exotic mesons is considered a favored production mode from the viewpoint of two-component duality.[1] Narrow X^{++} resonances might be produced with cross sections as large as $\sim 1\ \mu b$ in this reaction at our incident momentum of 8.4 GeV/c according to the model. We investigated the even G-parity decay modes $X^{++} \rightarrow \pi^+\pi^+$, $\pi^+\pi^+\pi^+\pi^-$, $\pi^+\pi^+\pi^+\pi^+\pi^-\pi^-$ and found no evidence for narrow, ~ 100 MeV, resonances having mass ≤ 3.0 GeV with cross section $\gtrsim 1 - 2\ \mu b$. Moreover, no evidence for a $\bar{p}p\pi^+\pi^+$ decay mode at the $1\ \mu b$ level is seen either.

We acknowledge with pleasure the enthusiastic assistance of the many people in the Stanford Linear Accelerator Center community who made this exotic meson search a reality. In particular, we wish to thank Roger Coombes and Robert Watt and his staff. In addition, we are deeply indebted to Anastasia Koshakji and her scanning staff at Vanderbilt University.

One of us (ECF) wishes to take this opportunity to thank Dr. Joseph Ballam for his hospitality during the early part of SLAC's development of the RCBC.

FOOTNOTES

* Since the hybrid system works best when the charged tracks in the bubble chamber have low momenta, we found that the best interpreted events were those where the forward neutron momentum is relatively large. In particular, when the forward neutron momentum is greater than 6 GeV/c, we found that the estimated number of events in each of the 2π, 4π and 6π final states, according to the missing mass calculation, the more restrictive 1C category, and the 3C category, are in substantial agreement.

** Note that the solid and dashed histograms are closer together at the low mass end of the spectrum. In this region the particle momenta are also low, resulting in more accurate measurements and fewer ambiguities.

*** We note that the triggering requirements and geometrical acceptance of our experiment are shown by the simulation program to have at least as great an effect on the particle distributions as the above matrix element. Comparisons of various distributions in the data with modified phase space matrix elements are given in a separate paper.[4]

REFERENCES

1. J. L. Rosner, The Classification and Decays of Resonant Particles, SLAC-PUB-1391, February 1974 (to be published in Physics Reports); M. Jacob and J. Weyers, Nuovo Cimento 69A, 521 (1970); 70A, 285 (1970); H. J. Lipkin, Phys. Rev. 7, 2262 (1973), Phys. Rev. 7, 237 (1973).
2. E. W. Anderson, et al., Phys. Rev. Letters 22, 1390 (1969).
3. NN and ND Interactions (above 0.5 GeV/c) -- A Compilation, Particle Data Group, UCRL - 2000 NN, August 1970; π^+p, π^+n, and π^+d Interactions, A Compilation: Parts I and II, Particle Data Group, LBL, May 1973.
4. M. S. Alam et al., A Study of Particle Spectra and Correlations in the Reaction $\pi^+ + p \to n(\text{forward}) + (2\pi, 4\pi, 6\pi)$ at 8.4 GeV/c, (Indiana-Purdue-SLAC-Vanderbilt Collaboration), VAND-HEP 74 (3).

FIGURE CAPTIONS

Fig. 1. Plan view of RCBC-Neutron Detector hybrid system.

Fig. 2. Pion effective mass spectra from events making 1C fits to n_{fwd} + pions.

Solid histograms contain 1C fits with the neutron momentum, $p_n \geq 3.0$ GeV/c, and with

a) χ^2 probability $\geq 4\%$ for $n_{fwd}\ \pi^+\pi^+$.

b) χ^2 probability $\geq 6\%$ for $n_{fwd}\ \pi^+\pi^+\pi^+\pi^-$.

c) χ^2 probability $\geq 6\%$ for $n_{fwd}\ \pi^+\pi^+\pi^+\pi^+\pi^-\pi^-$.

Dashed histograms are subject to the additional constraints:

a) $-1.0\ \text{GeV}^2 \leq MM^2 \leq 3.0\ \text{GeV}^2$.

b) The neutron + pions final state gives the best χ^2 probability and the next best fit has a probability at least a factor of 10 lower.

Fig. 3. Upper limits to the cross section for the production of narrow (< 100 MeV) exotic resonances decaying into 2, 4, and 6 pions.

Fig. 4. Pion effective mass spectra from events making 3C fits to n_{fwd} + pions with $p_n \geq 3.0$ GeV/c and with

a) χ^2 probability $\geq 2\%$ for $n_{fwd}\ \pi^+\pi^+$.

b) χ^2 probability $\geq 5\%$ for $n_{fwd}\ \pi^+\pi^+\pi^+\pi^-$.

c) χ^2 probability $\geq 2\%$ for $n_{fwd}\ \pi^+\pi^+\pi^+\pi^+\pi^-\pi^-$.

The solid curves are generated by the modified phase space model described in the text.

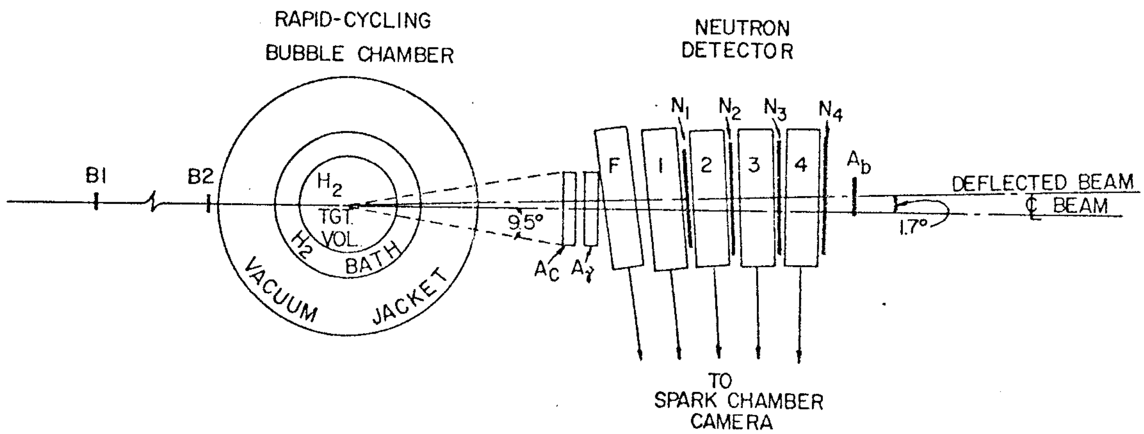
RAPID-CYCLING
BUBBLE CHAMBER
NEUTRON
DETECTOR
B1
B2
H2
TGT.
VOL.
H2 BATH
VACUUM JACKET
9.5°
AC
Aγ
F
1
2
3
4
N1
N2
N3
N4
Ab
DEFLECTED BEAM
℄ BEAM
1.7°
TO
SPARK CHAMBER
CAMERA

Fig. 1

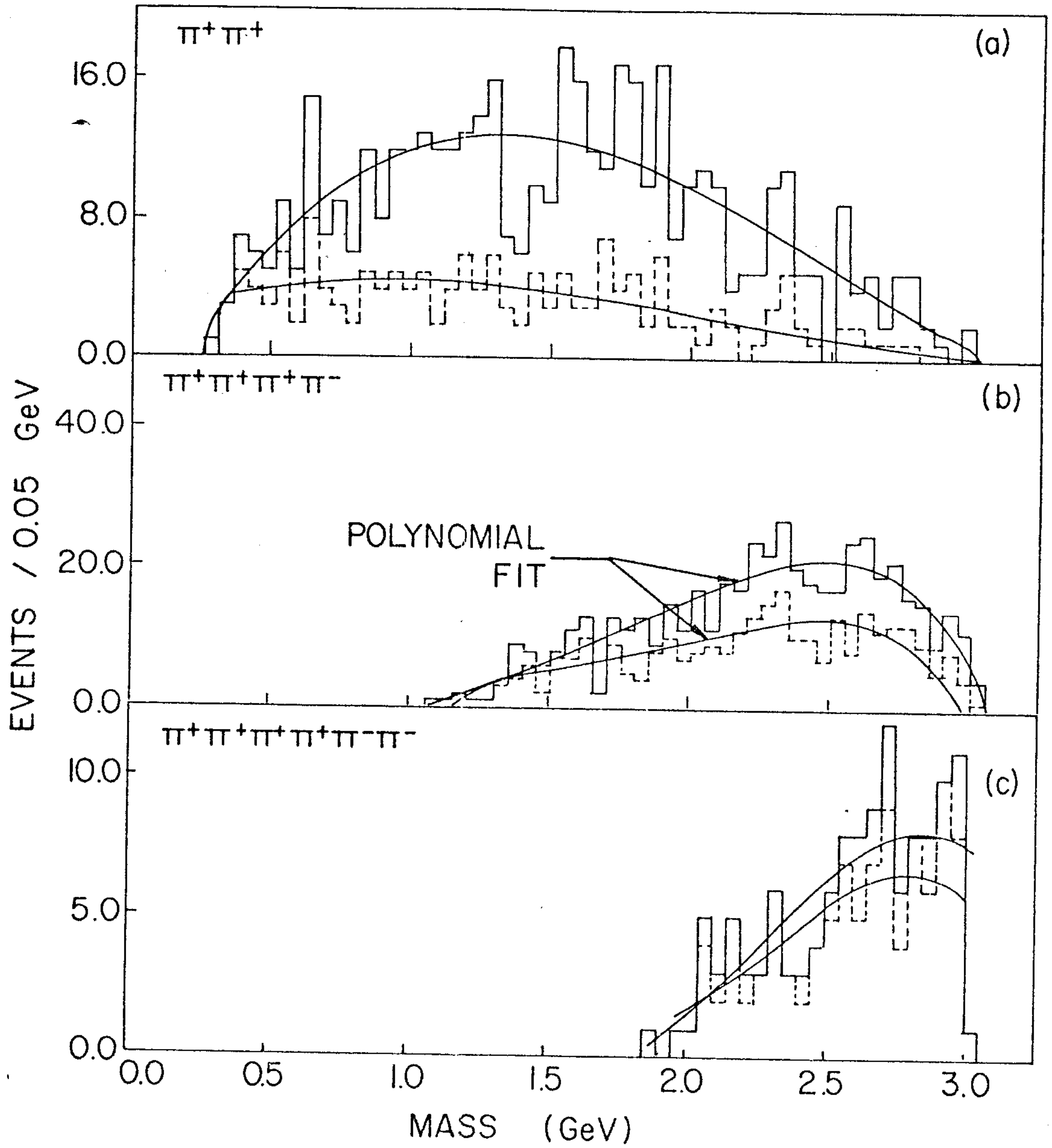

π⁺π⁺
(a)
16.0
8.0
0.0
π⁺π⁺π⁺π⁻
(b)
40.0
POLYNOMIAL
FIT
20.0
0.0
π⁺π⁺π⁺π⁺π⁻π⁻
(c)
10.0
5.0
0.0
EVENTS / 0.05 GeV
0.0
0.5
1.0
1.5
2.0
2.5
3.0
MASS (GeV)

Fig. 2

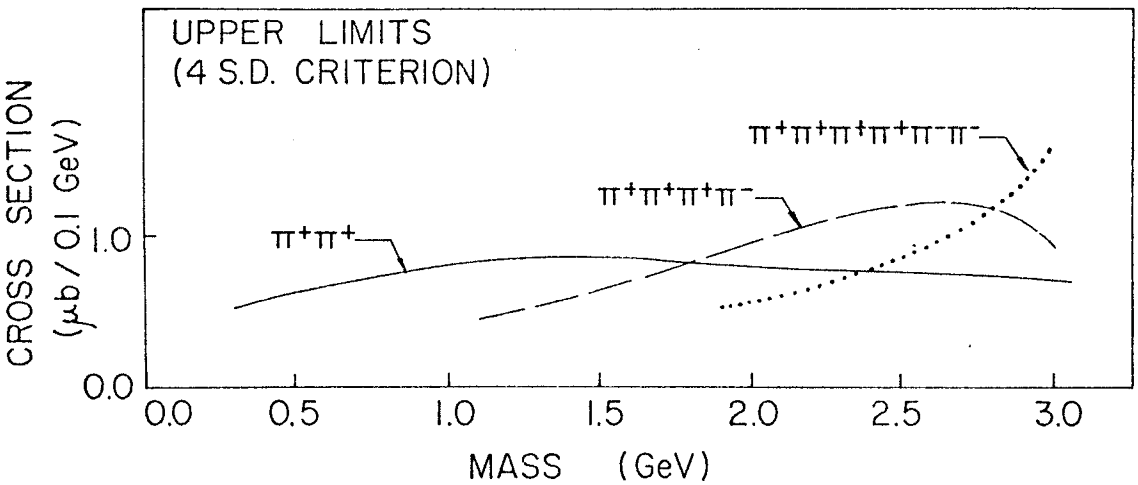
UPPER LIMITS
(4 S.D. CRITERION)
π⁺π⁺π⁺π⁺π⁻π⁻
π⁺π⁺π⁺π⁻
π⁺π⁺
CROSS SECTION
(μb / 0.1 GeV)
1.0
0.0
0.0
0.5
1.0
1.5
2.0
2.5
3.0
MASS (GeV)

Fig. 3

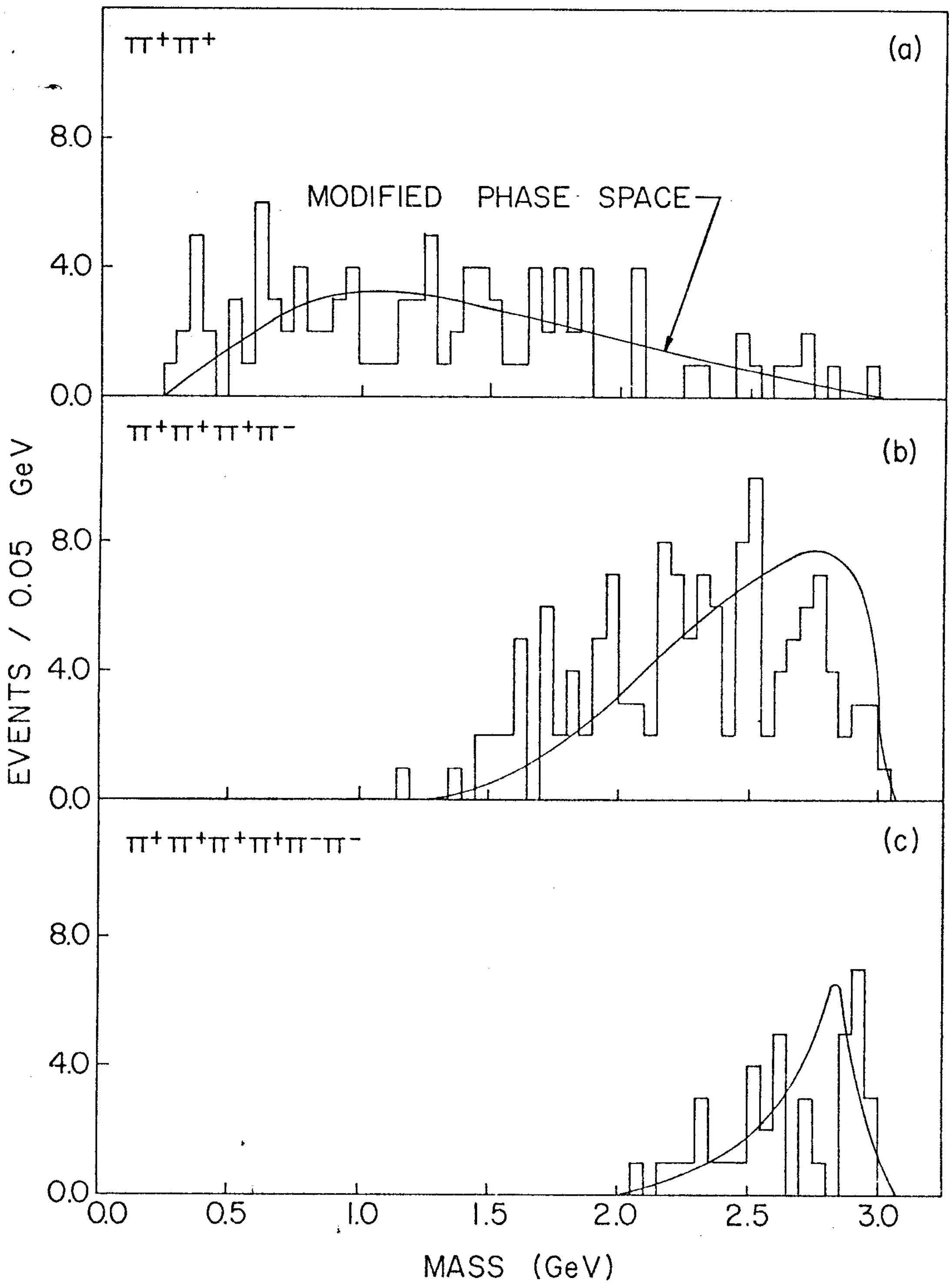

π⁺π⁺
(a)
MODIFIED PHASE SPACE
π⁺π⁺π⁺π⁻
(b)
π⁺π⁺π⁺π⁺π⁻π⁻
(c)
EVENTS / 0.05 GeV
0.0
4.0
8.0
0.0
0.5
1.0
1.5
2.0
2.5
3.0
MASS (GeV)

Fig. 4